Available online at www.sciencedirect.com

ScienceDirect

Ceramics International 40 (2014) 3847–3853

CERAMICS INTERNATIONAL

www.elsevier.com/locate/ceramint

# Microstructure and electrical conductivity of Mo/TiN composite powder for alkali metal thermal to electric converter electrodes

Sun-Dong Kim*, Se-Young Kim, Jong Hoon Joo, Sang-Kuk Woo

*Energy Materials and Convergence Division, Korea Institute of Energy Research, 152 Gajeongro, Yuseonggu, Daejeon 305–343, Republic of Korea*

Received 11 June 2013; received in revised form 6 August 2013; accepted 6 August 2013
Available online 15 August 2013

**Abstract**

A Mo/TiN composite powder has been synthesized by a sol–gel method to improve the electrical performance and microstructural stability of the alkali metal thermal to electric converter electrode. The core (TiN)–shell (Mo) structure of the composite powder is confirmed by energy-dispersive X-ray spectroscopy and scanning electron microscopy. The composite powder is primarily composed of submicron (400–800 nm) particles that are coated on a core ( > 3–5 μm) particle. The Mo/TiN composite electrode exhibits high electrical conductivities of 1000 $Scm^{-1}$ at 300 °C and 260 $Scm^{-1}$ at 700 °C in an Ar atmosphere. The electrode exhibits excellent tolerance against grain growth during thermal cycling tests (R.T. ↔ 800 °C), where the average growth rate of Mo grains in the Mo/TiN composite electrodes is controlled less than 0.5%/time (0.62 → 0.65 μm), while the growth rate in Mo electrodes is 306.7%/time (0.24 → 3.92 μm). It can be concluded that the Mo/TiN composite powder will suppress the degradation of the electrode and enhance the performance and durability of the unit cell at elevated temperatures.
© 2013 Elsevier Ltd and Techna Group S.r.l. All rights reserved.

*Keywords:* A. Grain growth; Alkali metal thermal to electric converter; Mo/TiN composite; Core-shell; Thermal cycling

## 1. Introduction

The alkali metal thermal to electric converter (AMTEC) is one of the most promising energy conversion devices that generate electricity from heat energy. Theoretically, an AMTEC system operates continuously without refueling using the sodium circulation in a beta"-alumina solid electrolyte (BASE) and a porous wick. The driving forces of this sodium circulation are the capillary force of the porous wick and the sodium pressure/activity difference between the Na evaporation region (600–800 °C) and the Na condensation region (200–400 °C). Due to the high efficiency, low manufacturing cost, light weight and static operation, the AMTEC system was once considered for use as a space power source [1–3]. However, there have been some problems associated with its durability during continuous operation. Causes of power loss in an AMTEC system include the increase in electrode polarization due to grain growth and the evaporation of the electrode material at high temperatures [4–8]. Thus, the development of a high performance, highly durable electrode is very important for AMTEC research.

Up till now, thin and porous Mo electrodes have shown the best performance as AMTEC electrodes [9–11]. This result is due to the formation of Na–Mo–O compounds, which might be responsible for the enhancement of Na transport through the Mo electrode. However, from the work of Williams et al. [11], it is confirmed that this compound evaporated at temperatures above 800 °C, resulting in the degradation of the electrode performance. To develop better electrode materials for use at high temperatures, Nakata et al. [12] investigated the reactivity of a ceramic electrode with liquid sodium, and TiN, TiC, NbN and NbC were considered as candidates for the AMTEC electrode material [12–14]. Although TiN and TiC can be used for the AMTEC electrode, Mo is the best material by far in terms of the electrochemical performance and the activity with a Na vapor [12].

Thus, the aim of this research is to achieve an AMTEC electrode with high electrochemical performance and microstructural stability at high temperatures using a Mo/TiN composite

*Corresponding author. Tel.: +82 42 860 3328; fax: +82 42 860 3133.
*E-mail address:* amastra@kier.re.kr (S.-D. Kim).

0272-8842/$ - see front matter © 2013 Elsevier Ltd and Techna Group S.r.l. All rights reserved.
http://dx.doi.org/10.1016/j.ceramint.2013.08.025

powder. In order to get high electrical conductivity, the shell is considered to be composed of metallic Mo particles. The Mo/TiN composite powder offers the following advantages: (1) microstructural stability-sintering of the metallic (Mo) phase is controlled by the conjugated ceramic (TiN) phase, (2) high interfacial affinity with the BASE-wet processes (screen printing, dip-coating, etc.) can be used for electrode coating, (3) self-assembly of a porous microstructure without using a pore-former, (4) mixed homogeneity and (5) TiN and Mo supplementing effects.

## 2. Experimental

### 2.1. Synthesis of Mo/TiN composite powder

The synthesis procedure for the proposed Mo/TiN composite powder follows a sol–gel method that uses ethylenediaminetetraacetic acid (EDTA) as the chelating reagent, as depicted in Fig. 1 Titanium nitride (TiN, Aldrich) was used as the core material and synthesized molybdenum (Mo) was used to build the shell structure of the Mo/TiN composite powder. An aqueous solution of ammonium molybdate ($(NH_4)_6Mo_7O_{24}\cdot 4\,H_2O$), Aldrich) was mixed with EDTA (company) by stirring and heated at 80 °C for 3 h. TiN and ethylene glycol (EG, Junsei) were then added to the aqueous solution to synthesize a Mo polymeric solution. The polymeric solution was condensed at 180 °C for 2 h and an ash-colored intermediate was obtained. The resulting intermediates were calcined at 500 °C for 3 h in air and then re-heated at 900 °C for 6 h in $H_2$ 5%/Ar 95%. The synthesized powders were milled in methanol overnight and dried in a convection oven. Finally, the Mo/TiN composite powders were obtained by sieving the dried powder.

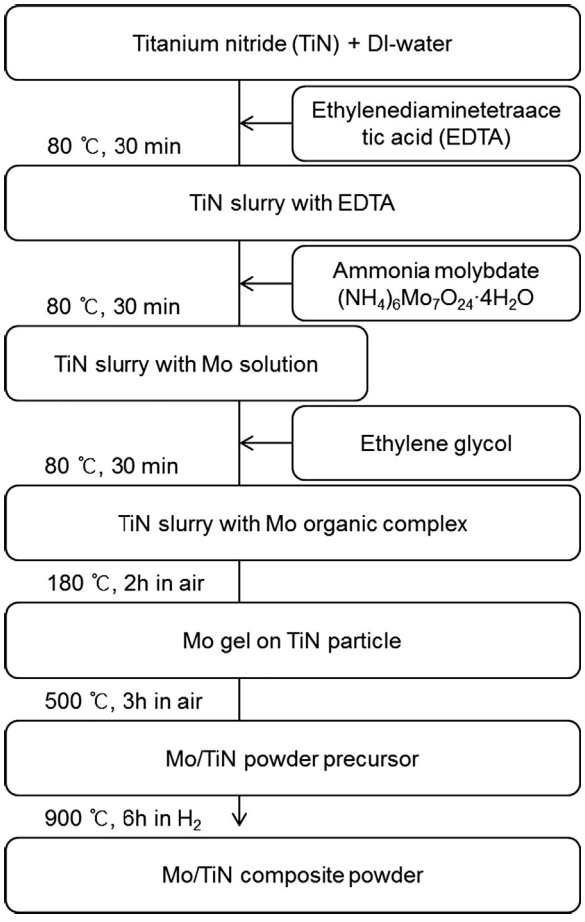


Fig. 1. Experimental flow chart for the synthesis of Mo/TiN composite powders.

### 2.2. Characterizations of Mo/TiN composite powder

The crystalline phases of the synthesized powders were analyzed using X-ray diffraction (Rint 2700, Rigaku Co., Japan). The microstructures of the Mo/TiN powder were visualized by field emission scanning electron microscopy (FESEM, model S4200, Hitachi Ltd., Japan). The regional elements of the composite powder were investigated using energy dispersive X-ray spectroscopy (EDX) with the same instrument (FESEM, model S4200, Hitachi Ltd., Japan). The electrical conductivity of the TiN–Mo electrode was measured using the DC-4 probe method. The grain size of the Mo powder was evaluated by measuring the average diameter of 10 random grains (see Fig. 9) on the primary particles in the SEM images. The grain growth of the electrode powder was evaluated via thermal cycling tests with temperatures ranging from room temperature (R.T.) to 800 °C in an Ar atmosphere.

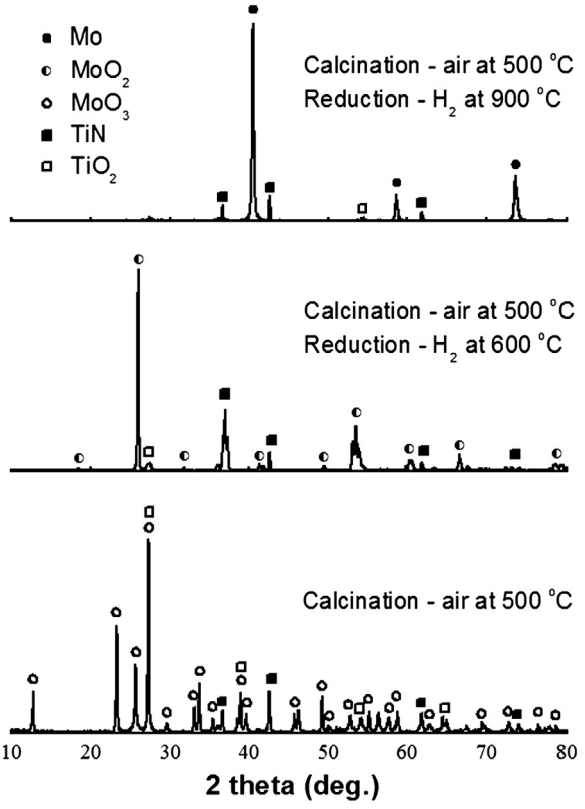


Fig. 2. X-ray diffraction patterns of Mo/TiN composite powders with different synthesis procedures.

## 3. Results and discussion

The crystalline phases of the Mo/TiN composite powders, which depend on the synthesis procedures, are shown in Fig. 2. By heat treating the Mo/TiN powder precursor at 500 °C in air, most of the elements formed oxides. Molybdenum is predominantly oxidized to $MoO_3$, and even TiN is partially oxidized to $TiO_2$. The powder gradually loses its oxygen bonding with increasing temperature in a hydrogen atmosphere. At 600 °C, every $MoO_3$ phase is transformed into $MoO_2$, and the $TiO_2$ phase is also reduced. The metallic Mo phase and TiN phase could be obtained at 900 °C in a hydrogen atmosphere. As described in the experimental (Section 2.1), the starting material for making the core of the Mo/TiN composite particle is a commercial TiN (Aldrich). During the synthetic process, the surface of the core particle is partially oxidized to $TiO_2$. After that, the $TiO_2$ layer has been reduced to $TiO_x$ ($x < 2.0$) phases and the stoichiometry index "$x$" has been decreased depending on the reducing environment (i.e. temperature and gas environment). The shapes of the powders varied depending on the crystalline phases, as shown in Fig. 3. Before reduction, $MoO_3$ polyhedrons and TiN (or $TiO_2$) are mixed together randomly. During the reduction process, the Mo grain size decreased dramatically at elevated temperatures, and the platelike polyhedrons decomposed at the same time. Finally, the Mo/TiN composite powder was synthesized at 900 °C with a porous structure. The grain size of the primary particles is only a few hundred nanometers even though the size of the agglomerates is on the micron scale. When considering the function of the electrode, the microstructure of this composite powder is very desirable due to the high surface area on the microscale and the high porosity on the macroscale.

Fig. 4 shows the core-shell structure of the Mo/TiN composite powder, which was confirmed by SEM and EDX. We intentionally found an incomplete particle, which shows a bare surface and a coated surface simultaneously. The configuration of the powder consists of primarily submicron (=400–800 nm) particles coated on a core (> 3–5 μm) particle. The bare surface (region ⓑ) in Fig. 4a, which forms the core, is confirmed to be TiN by EDX analysis (Fig. 4b). Most of the TiN particles are fully covered by porous Mo particles. The results shown in Fig. 4c imply that most of the region ⓒ is composed of Mo particles and that the coating layer is thin and porous, taking into account the information depth and area of EDX.

The crystalline phases of the Mo/TiN composite powders, which are dependent on the synthesis conditions, are shown in Fig. 5. The only variable is the heating temperature; the dwelling time (6 h) and gas atmosphere (95% Ar/5% $H_2$) are fixed. There still exist $TiO_2$ and $MoO_2$ as intermediates with the Mo and TiN phases at 800 °C. These oxides are completely eliminated above 900 °C, and Mo does not form any secondary phases with Ti or N. Fig. 6 shows the microstructures of the Mo/TiN composite powder for different synthesis temperatures. The powder in Fig. 6a and d is incomplete because the shape and size of the powder is irregular and the Mo grain on the surface is still immature. However, the powder showed a uniform and porous microstructure above 900 °C, and the pore structure of the powder showed a minute change at elevated temperatures.

The SEM micrographs of the electrodes, which are made from the Mo with a beta"-alumina mixture and from the Mo/TiN composite powder, are depicted in Fig. 7. Mo and TiN are the most promising materials for the AMTEC electrode [9–11]. Despite the high electrical conductivity of the Mo electrode, the

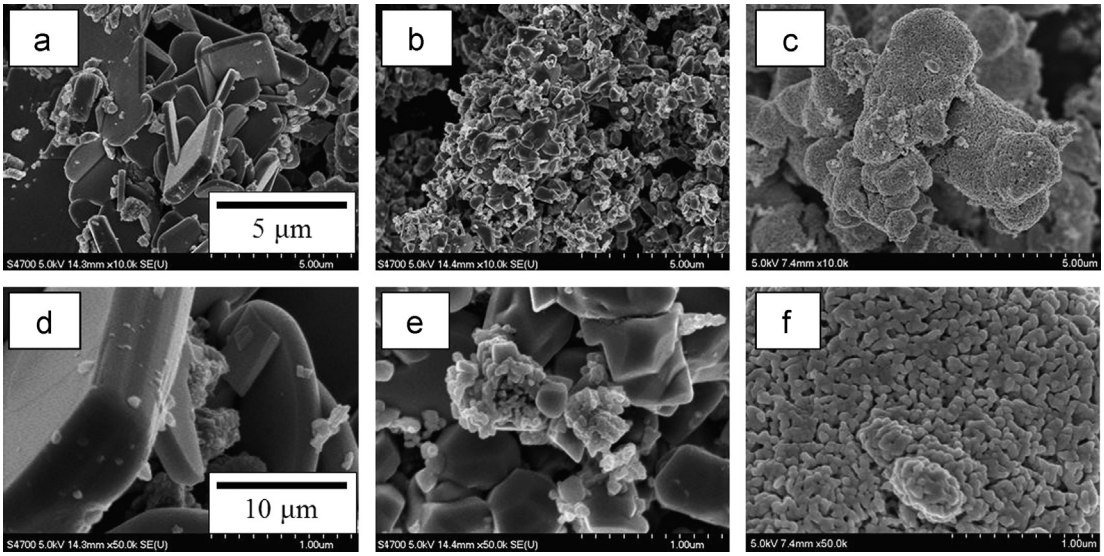


Fig. 3. SEM micrographs of Mo/TiN composite powders with different synthesis procedures: (a) calcined in air at 500 °C ( × 10 k image), (b) reduced in $H_2$ at 600 °C after being calcined in air at 500 °C ( × 10 k image), (c) reduced in $H_2$ at 900 °C after being calcined in air at 500 °C ( × 10 k image), (d) calcined in air at 500 °C ( × 50 k image), (e) reduced in $H_2$ at 600 °C after being calcined in air at 500 °C ( × 50 k image) and (f) reduced in $H_2$ at 900 °C after being calcined in air at 500 °C ( × 50 k image).

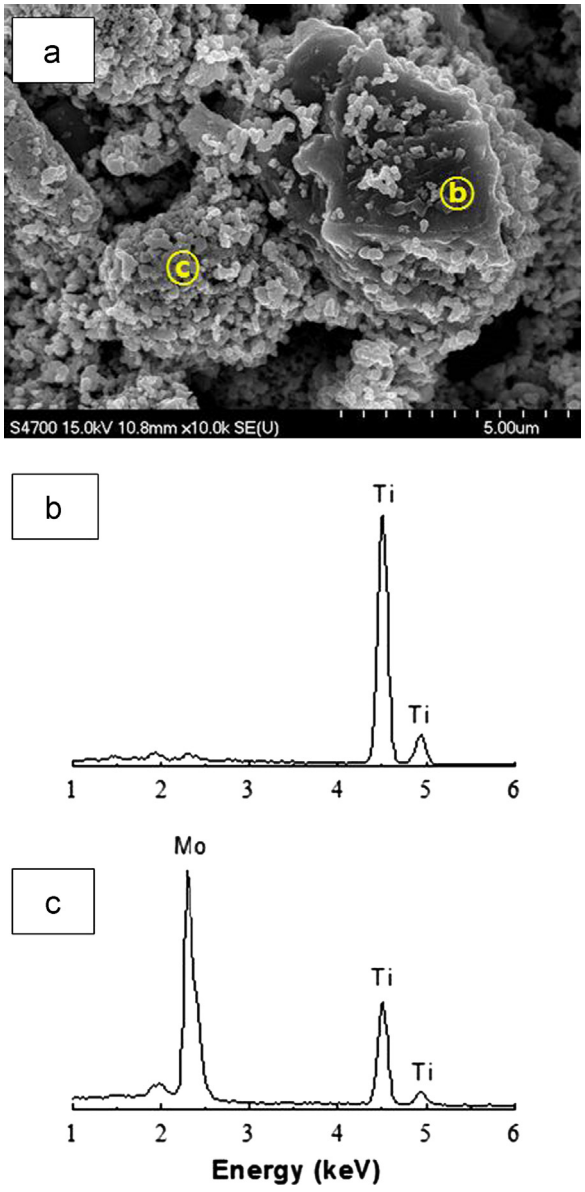


Fig. 4. (a) SEM micrographs of the Mo/TiN core-shell structure, (b) the EDX signal used to analyze the elements in region ⓑ and (c) the EDX signal used to analyze the elements in region ⓒ.

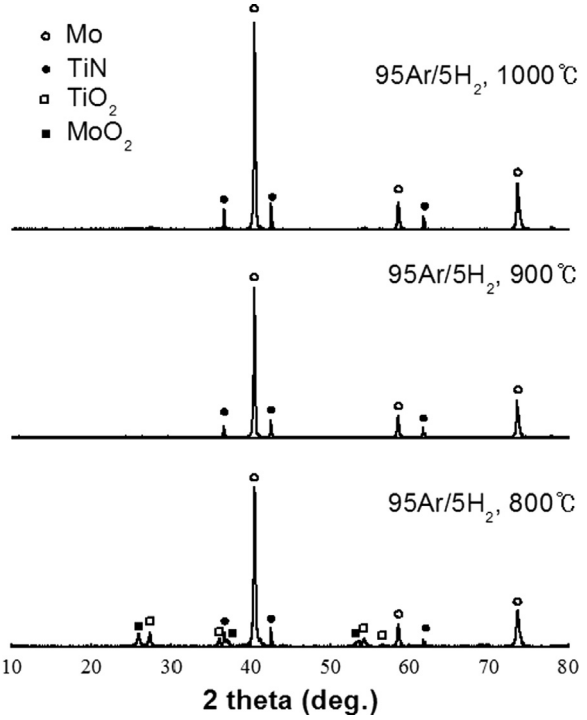


Fig. 5. X-ray diffraction patterns of Mo/TiN composite powders with different synthesis temperatures in a 95 Ar/5 $H_2$ atmosphere.

thermal expansion coefficient (TEC) mismatch between Mo ($5.43 \times 10^{-6}$/°C) and the BASE ($7.2–8.6 \times 10^{-6}$/°C) is a fundamental problem. For this reason, the manufacturing of the Mo electrode is limited to a few processing methods, including chemical vapor deposition (CVD), sputtering or thermal plasma coating, which are very expensive and have many geometry restraints [15]. In our research, we tried to develop a wet process, e.g., dip-coating, slurry spray-coating, etc., for manufacturing the Mo electrode. As shown in Fig. 7a, the Mo electrode is delaminated from the alumina substrate even with the addition of 20 vol% of the beta"-alumina powder, which is the electrolyte material. By increasing the concentration of the beta"-alumina powder, the adhesion between alumina and the electrode improved significantly, and there was no delamination in the interface (Fig. 7b). In the case of the Mo/TiN composite powder, the interface was well organized, and there was no delamination even after the electrochemical measurement. More importantly, the porous structure with the combination of micropores and macropores, which is shown in Fig. 7c, achieves a sufficient sodium flow and has a large enough three phase boundary (TPB) for a highly efficient electrochemical reaction.

The electrical conductivity of the various electrodes as a function of temperature is shown in Fig. 8. The Mo (Mo:BASE=9:1, 4:1 and 2:1 wt%) and Mo/TiN composite electrodes are prepared and every measurement is simultaneously performed in Ar. The BASE powder was added to the Mo electrode to increase its adhesion to the alumina substrate. The Mo (Mo:BASE=9:1 wt%) electrode exhibited the highest electrical conductivity within the scope of these experiments. However, as mentioned above, the Mo electrodes have a delamination problem; especially those with high Mo content (see Fig. 7a). The electrical conductivity of the Mo electrode decreased with increasing beta"-alumina concentration. The electrode made from the Mo/TiN composite powder exhibited high electrical conductivities of approximately 1000 $Scm^{-1}$ at 300 °C and 260 $Scm^{-1}$ at 700 °C. The compositional ratio of Mo:TiN in the Mo/TiN composite powder is 50:50 vol%. Even with the low Mo content, the electrode showed good electrical performance due to the effective percolation through the sides of the shells, i.e., the fine and porous Mo coating layer of the composite powder.

One of the main causes of performance degradation in an AMTEC system is the grain growth of the electrode [4–6]. Theoretical studies have shown that the TPB length in an electrode is inversely proportional to the grain size [16]. Due

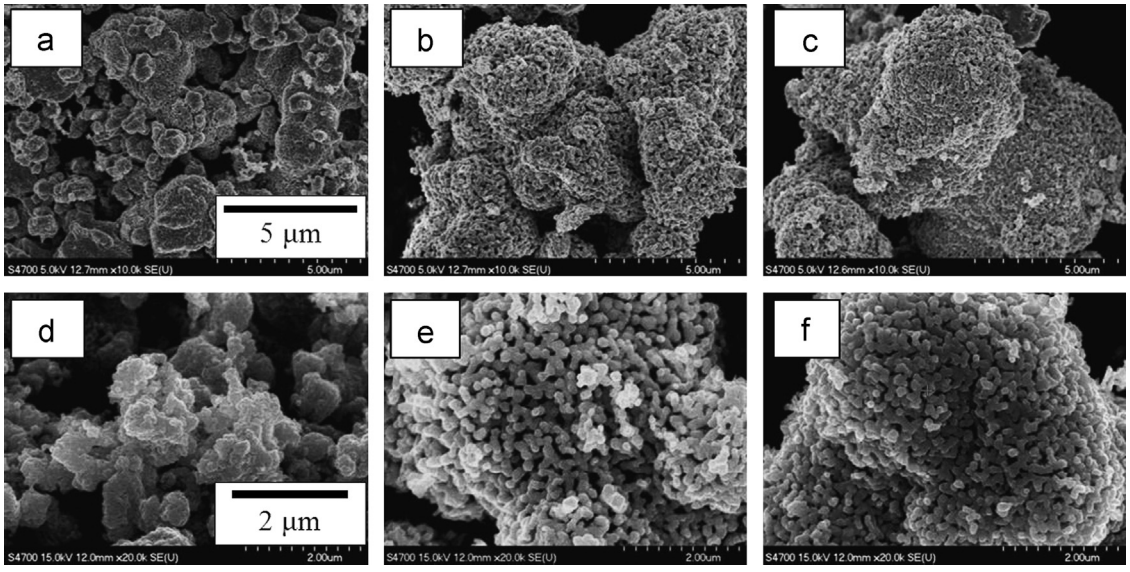


Fig. 6. SEM micrographs of Mo/TiN composite powders with different synthesis temperatures in a 95Ar/5 $H_2$ atmosphere: (a) 800 °C ( × 10 k image), (b) 900 °C ( × 10 k image), (c) 1000 °C ( × 10 k image), (d) 800 °C ( × 20 k image), (e) 900 °C ( × 20 k image) and (f) 1000 °C ( × 20 k image).

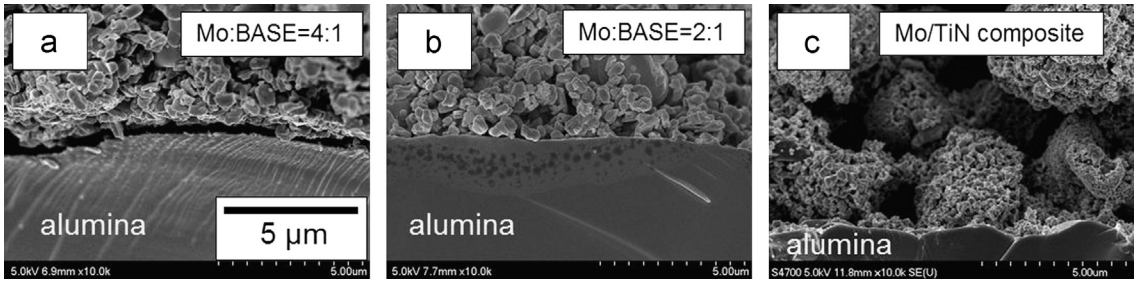


Fig. 7. SEM micrographs of the electrode/alumina interface: (a) Mo electrode (Mo:BASE=4:1 wt%), (b) Mo electrode (Mo:BASE=2:1 wt%) and (c) Mo/TiN composite electrode.

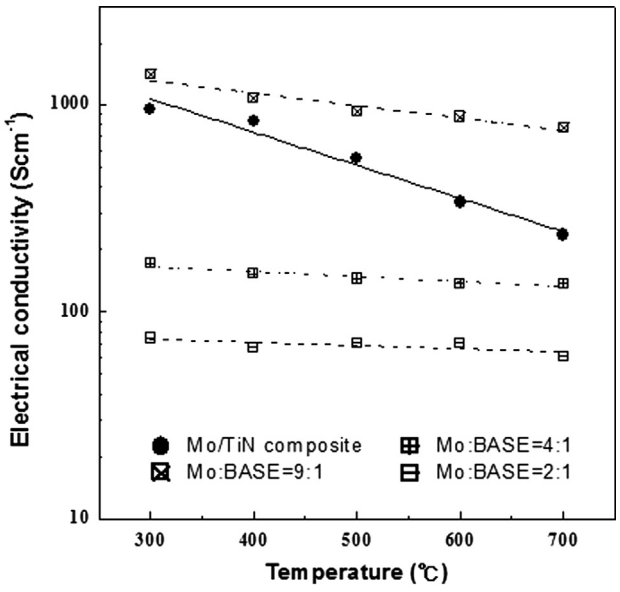


Fig. 8. Electrical conductivity of the electrodes as a function of temperature.

to the coarsening phenomena at elevated temperatures, the TPB length decreased in the electrode, and the efficiency of the electrochemical reaction also decreased. Fig. 9 shows the microstructural variations in the Mo/TiN electrode and Mo electrode for different numbers of thermal cycling tests (R.T. ↔ 800 °C). After each thermal cycling test, the average grain size of the electrode was measured using the SEM image. There is a stark contrast between the Mo/TiN composite powder (Fig. 9a–c) and Mo (Fig. 9d–f) in terms of grain growth. The grain size of the Mo particle grew proportionally to the number of thermal cycling tests. Conversely, there is little variation in the grain size of the Mo/TiN composite powder. The average grain size for each cycling test is summarized in Fig. 10. Initially, the Mo grain size (0.24 μm) is smaller than that of the Mo/TiN composite powder (0.62 μm), as shown in Fig. 9d. However, the Mo grain has grown larger due to the thermal cycling, and there is a rapid growth even for 2–3 thermal cycling tests. We cannot measure the grain growth after the 5th thermal cycling due to the disappearance of the Mo electrode. It is reasonable to assume that the missing of

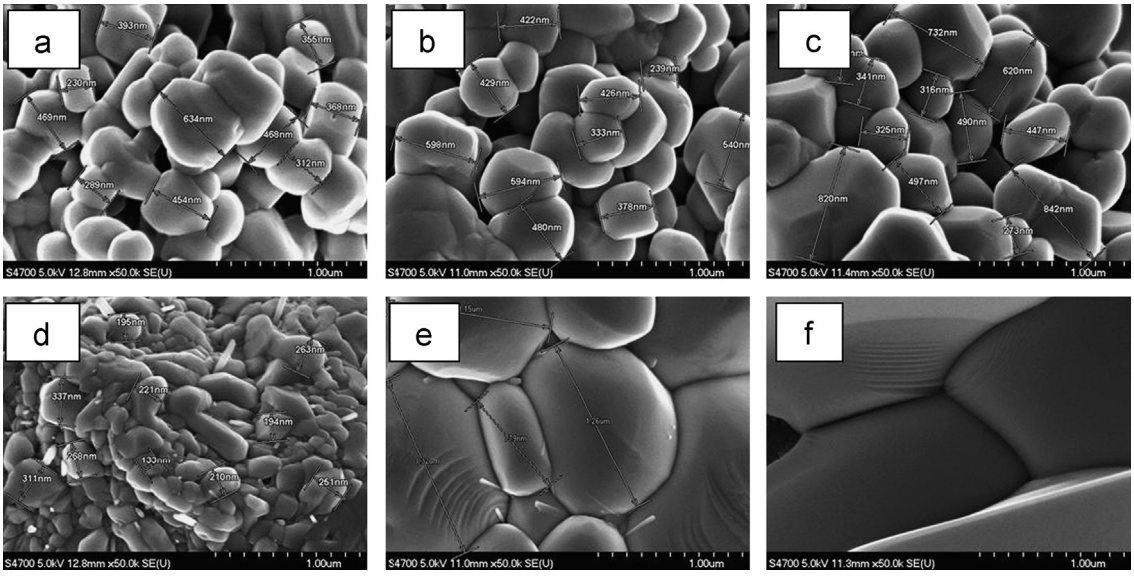


Fig. 9. SEM micrographs of Mo grains for different numbers of thermal cycling tests: (a) initial image of a Mo grain in a Mo/TiN composite electrode, (b) image of the Mo grain in the Mo/TiN composite electrode after the 3rd thermal cycling, (c) image of the Mo grain in the Mo/TiN composite electrode after the 5th thermal cycling, (d) initial image of a Mo grain in a Mo electrode, (e) image of the Mo grain in the Mo electrode after the 3rd thermal cycling and (f) image of the Mo grain in the Mo electrode after the 5th thermal cycling.

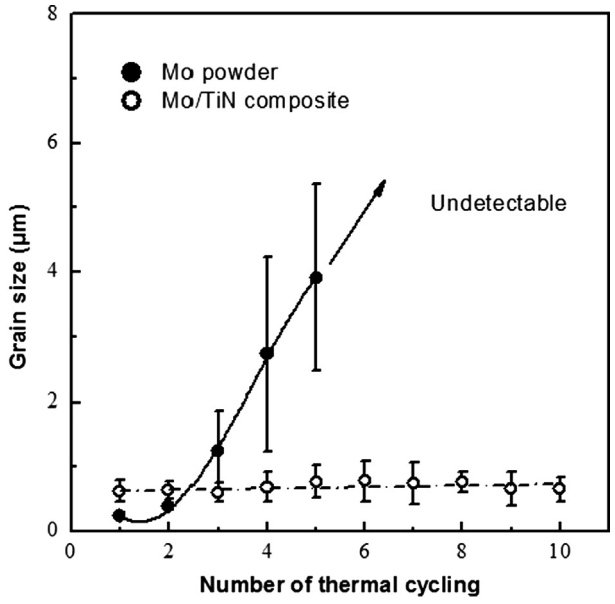


Fig. 10. Grain size variations in the electrodes for different numbers of thermal cycling tests.

electrode is due to the grain growth of the Mo particle. At elevated temperatures, the grain size increased rapidly, which led to a decrease in the number of grains and to a decrease in the contact area between the electrolyte and electrode. As the contact area decreased, the particles are easily detached from the electrode, and, moreover, the decrease in the contact area between the electrode and electrolyte can increase the interfacial resistance. During the thermal cycling test, the average growth rate of the Mo/TiN composite powder was 0.5%/time (0.62 → 0.65 μm) and of Mo was 306.7%/time (0.24 → 3.92 μm).

From these results, it is confirmed that the functional Mo/TiN composite powders effectively suppress the grain growth at elevated temperature. As a similar work of Kim et al., it could be interpreted that it is due to the formation of the $TiO_x$ intermediate layer between the core TiN and the Mo shells [17]. Each materials share in common with the intermediate layer by forming the -Ti–O–Mo- bonding structure. The bond enthalpy of the -Mo–O- diatomic species is $560.2 \pm 20.9$ kJ $mol^{-1}$ [18]. Even the chemical bonds have little influence on the overall crystalline structure, there need higher energies over the bond enthalpy in order to break the attraction between the Mo and TiN interfaces.

## 4. Conclusions

The current study investigated the electrical conductivity and microstructural stability of the AMTEC electrode that is made from a Mo/TiN composite powder. The composite powder is primarily composed of submicron (=400–800 nm) particles that are crystallized on a core (> 3–5 μm) particle surface and was successfully synthesized by a sol–gel method with EDTA as the chelating reagent. The interfacial affinity between the alumina substrate and Mo/TiN composite electrode is significantly improved compared with that of the Mo electrode. The electrode made from the Mo/TiN composite powder exhibited high electrical conductivities of 1000 $Scm^{-1}$ at 300 °C and 260 $Scm^{-1}$ at 700 °C, even with a reduced Mo content (50 vol%). The Mo/TiN composite electrode exhibited excellent tolerance against grain growth at elevated temperatures. The average growth rate of the Mo grains in the Mo/TiN composite electrodes was controlled and less than 0.5%/time (0.62 → 0.65 μm), while the growth rate in the Mo electrodes was 306.7%/time (0.24 → 3.92 μm) during the thermal cycling

tests. From these results, it can be concluded that the Mo/TiN composite powder has very effective electrical properties and high-temperature stability.

## Acknowledgments

This work was conducted under the framework of Research an Development Program of the Korea Institute of Energy Research (B3-2436-01).

## References

[1] M.A.K. Lodhi, P. Viijayaraghavan, A. Daloglu, An overview of advanced space/terrestrial power generation device: AMTEC, Journal of Power Sources 103 (2001) 25–33.
[2] J.M. Tournier, M.S. El-Genk, Performance analysis of Pluto/Express, multitube AMTEC cells, Energy Conversion and Management 40 (1999) 139–173.
[3] S.Y. Wu, L. Xiao, Y.D. Coa, A review on advances in alkali metal thermal to electric converters (AMTECs), International Journal of Energy Research 33 (2009) 868–892.
[4] M.A.K. Lodhi, J.B. Briggs, Temperature effect on lifetimes of AMTEC electrodes, Journal of Power Sources 168 (2007) 537–545.
[5] M.A.K. Lodhi, M.S. Chowdhury, Characteristics of electrodes materials and their lifetime modeling for AMTEC, Journal of Power Sources 103 (2001) 18–24.
[6] M.A.K. Lodhi, S.C. Soon, M. Mohibullah, Temperature-dependent grain growth model for AMTEC electrodes, Journal of Power Sources 135 (2004) 304–310.
[7] M.A.K. Lodhi, M.S. Chowdhury, The role of electrodes in power degradation of AMTEC: analysis and simulation, Journal of Power Sources 96 (2001) 369–375.
[8] M.A.K. Lodhi, J.B. Briggs, The grain size effect on thermo-chemical properties of AMTEC electrodes, International Journal of Electrochemical Science 2 (2007) 469–477.
[9] K. Tanaka, Experimental evaluation of electrode conversion efficiency of alkali metal thermal to electric converter, Heat Transfer-Asian Research 30 (3) (2001) 234–244.
[10] H. Yokokawa, T. Horita, N. Sakai, T. Kawada, M. Dokiya, Chemical thermodynamic stabilities of electrode/electrolyte interfaces of high temperature electrochemical cells, Solid State Ionics 78 (1995) 203–210.
[11] R.M. Williams, G. Nagasubramanian, S.K. Khanna, C.P. Bankston, A.P. Thakoor, T. Cole, The role of oxygen in porous molybdenum electrodes for the alkali metal thermoelectric converter,, Journal of The Electrochemical Society 133 (8) (1986) 1587–1595.
[12] H. Nakata, T. Nagata, K. Tsuchida, A. Kato, Ceramic electrodes for an alkali metal thermo-electric converter (AMTEC), Journal of Applied Electrochemistry 23 (1993) 1251–1258.
[13] K. Tsuchida, T. Nagata, H. Nakata, A. Kato, $LaB_6$ and $TiB_2$ electrodes for the alkali metal thermoelectric converter, Journal of Materials Science 33 (1998) 755–762.
[14] Q. Fang, Q. Knodler, Porous $TiB_2$ electrode for the alkali metal thermo-electric convertor, J. Mater. Sci (1992) 3725–3729.
[15] H. Mukunoki, O. Fukumasa, S. Sakiyama, Integrated synthesis of AMTEC electrode by using controlled thermal plasma processing, Thin Solid Films 407 (2002) 92–97.
[16] X. Deng, A. Petric, Geometrical modeling of the triple-phase-boundary in solid oxide fuel cells, Journal of Power Sources 140 (2005) 297–303.
[17] S.D. Kim, H. Moon, S.H. Hyun, J. Moon, J. Kim, H.W. Lee, Performance and durability of Ni-coated YSZ anodes for intermediate temperature solid oxide fuel cells, Solid State Ionics 177 (2006) 931–938.
[18] D.R. Lide, Handbook of Chemistry and Physics, 79th edition, CRC press, Boca Raton, USA, 1998.